ONR TECHNICAL REPORT
JWTR-3

"The Relationship Between the Microstructure
and Age Hardening Response in the Metastable
Beta Titanium Alloy Ti-11.5Mo-6Zr-4.5Sn (Beta III)"

Department of Metallurgy and Materials Science
Carnegie-Mellon University
Pittsburgh, PA 15213

August 1977

"The Relationship Between the Microstructure
and Age Hardening Response in the Metastable
Beta Titanium Alloy Ti-11.5Mo-6Zr-4.5Sn (Beta III)"

N00014-76-C-0409

Department of Metallurgy and Materials Science
Carnegie-Mellon University
Pittsburgh, PA 15213

August 1977

(See 1473)

THE RELATIONSHIP BETWEEN MICROSTRUCTURE AND AGE
HARDENING RESPONSE IN THE METASTABLE BETA TITANIUM
ALLOY TI-11.5Mo-6Zr-4.5Sn (BETA III)

F. H. Froes*, C. F. Yolton*, J. M. Capenos*,
M. G. H. Wells*and J. C. Williams≠

ABSTRACT

The influence of heat treatment and oxygen content on the aging
response and microstructure of the metastable β-phase titanium alloy
Ti-11.5Mo-6Zr-4.5Sn (Beta III) has been studied using light and electron
metallography and hardness measurements. Increasing the oxygen from 0.17
to 0.28 wt% was shown to suppress ω-phase formation and accelerate α-phase
formation. Changing the solution treatment from above to below the β transus
was shown to significantly increase the rate of α-phase formation at residual disloca-
tions and sub-boundaries present in the warm worked material. Direct aging
has been shown to greatly retard the rate of ω-phase formation by comparison
to quenching and aging. Duplex aging first at a temperature in the ω-phase
formation range and then at a temperature in the α-phase formation range
results in a very fine dispersion of α-phase particles and a very high hard-
ness. It is suggested that this α-phase forms by an in-situ ω→α transformation.
In quenched samples small amounts (10%) of cold work was shown to accelerate
the formation of ω-phase during subsequent aging as shown by both electron
microscopy and by hardness measurements. Finally, some remarks are included
to indicate the application of our observations to the commercial heat treatment
of β-III.

*Colt Industries, Crucible Materials Research Center, Pittsburgh, PA
≠ Carnegie-Mellon University, Pittsburgh, PA

INTRODUCTION

There recently has been renewed interest in the class of Ti alloys known as β-alloys, or more properly, metastable β alloys. As a result, several new alloys have been developed.[1] The metastable β alloys have numerous advantages, among these are cold formability, potential for high strength with good fracture toughness and deep hardening characteristics. In this context deep hardening means that the kinetics of formation of the strengthening precipitate are sluggish enough that uniform properties can be obtained in thick (deep) sections. Thus these alloys have the potential for developing good combinations of strength and toughness for large components. In addition, they are readily fabricated into sheet and such sheet exhibits good ductility in sheet forming applications.

The constitution of the metastable β alloys is relatively complex and depends both on alloy composition and on aging temperature. The decomposition of the metastable β-phase has recently been reviewed,[2] thus, we will only give a brief summary of the decomposition behavior. In addition to two types of α-phase which can form during β-phase decomposition,[3] there are two transition phases: the b.c.c., solute-lean β-phase[4] and the hexagonal, solute-lean ω-phase.[5-7] The former of these transition phases forms in alloys which are more heavily β-stabilized than those which form ω-phase. Further, processing histories which result in a high density of heterogeneous nucleation sites such as an increased dislocation densities or sub-boundaries promote direct α-phase formation without the formation of transition precipitates. It is generally acknowledged that ω-phase formation leads to severe ductility losses[8,9] although it has been shown that proper control of the ω-phase volume fraction can lead to high strength with reasonable ductility.[9] It has also been suggested that controlling ω-phase volume

fraction maybe too difficult to be commercially feasible. Uncontrolled ω-phase formation leads to unacceptable ductility.[10] Thus the commercial heat treatments of β-alloys are designed to avoid ω-phase formation.

We have studied the relationship between microstructure and hardening response in a metastable β-phase alloy, Ti-11.5Mo-6Zr-4.5Sn, known as Beta III. Earlier studies have shown that this alloy can be heat treated to develop very high hardness and strength up to 1400 MN/m^2 (∿ 200 ksi).[11-13] This alloy can be solution heat treated to retain the β-phase and is very cold formable in the solution-treated condition. Alternatively, the alloy can be solution-treated and aged to form the α-phase or the ω-phase and these conditions result in the high strength levels mentioned above. Further, the role of oxygen in altering the age-hardening kinetics has been examined by studying material of two different oxygen levels.

MATERIALS AND EXPERIMENTAL METHODS

Alloys of similar composition except for oxygen were studied. The oxygen levels of the alloys were 0.17 and 0.28 wt%, the former representing normal commercial material, the latter a special high oxygen heat used for experimental purposes only. These alloys will be called low oxygen and high oxygen henceforth. The chemical analysis of these two alloys is given in Table I. After primary ingot breakdown, slabs were rolled from 1925°F (∿ 1050°C) to 0.180 inch (4.6mm) thick hot band. The hot band was then box annealed for eight hours at 1200°F (∿ 650°C) and furnace cooled. This material was finally cold rolled ∿ 10% in the laboratory prior to solution treatment.

All solution annealing was carried out in an air furnace while aging was undertaken in salt baths. Specimens for structure studies were prepared by standard metallographic procedures and etched in a dilute nitric acid - flourosilicic

acid - ammonium biflouride solution. This etchant proved to relatively slow and easy to control, requiring between 15 and 90 seconds etching time depending on the heat treatment of the sample. Uranium shadowed plastic replicas were used for replica electron microscopy. Thin foils were prepared by methods previously described.[14,15] X-ray diffraction identification of phases was carried out by the powder method using small needle samples prepared from heat treated bulk material.

RESULTS AND DISCUSSION

We have examined the effect of oxygen content, aging temperature, duplex aging, direct aging, cold work prior to aging and solution treatment temperature (relative to the β-transus) on the hardening response of the β-III alloy. The results will be reported and discussed separately for each of these variables.

Oxygen Effects

The effect of oxygen on aging response has been studied in materials of two oxygen levels which were solution treated both above (supra) and below (sub) the β-transus. The as-solution treated hardnesses for the two oxygen levels are markedly different as can be seen from Figure 1. Thin foil electron microscopy examination of the as-solution-treated materials showed the athermal ω-phase was present as a uniform dispersion of small (30-40A) particles. This is illustrated by selected area diffraction pattern and dark field micrograph of Figure 2. The influence of oxygen on the as-quenched hardness is somewhat difficult to interpret because of the presence of this athermal ω-phase, although we suggest that the increased hardness of the higher oxygen material results from solid solution hardening due to oxygen rather than a variation in the amount of ω-phase.

- 3 -

This interpretation is based on the earlier results of Paton and Williams,[16] who showed that increasing oxygen suppresses athermal ω-phase formation. Thus if the principal effect of oxygen is alteration of the athermal ω-phase volume fraction, the as-quenched hardnesses of the lower oxygen material would be higher. The opposite is observed.

Aging the solution-treated materials at 700°F ($\sim 370^{\circ}$C) results in substantial increases in hardness in the materials of both oxygen contents, although the rate of hardness increase is distinctly more rapid in the low oxygen material. This also can be seen from Figure 1,which also shows that an incubation period is observed in the high oxygen material before a hardness increase occurs. Thin foil electron microscopy has showed that 700°F ($\sim 370^{\circ}$C) aging of both materials results in the formation of isothermal ω-phase. Examples are shown in Figure 3. Aging for 500 hours at 700°F ($\sim 370^{\circ}$C) results in coarsening of the ω-phase, as can be seen by comparing the ω-phase particle size in Figure 3(a) and (b). This accounts for the overaging observed after extended aging periods.

Aging at temperatures of 900°F ($\sim 480^{\circ}$C) and above, results in formation of the equilibrium α-phase. This phase forms as elongated plates or needles, the long dimension of which lies along $\langle 110 \rangle_{\beta}$. The hardness-time curves, Figure 4, show that aging times greater than ~ 10 minutes at 900°F ($\sim 480^{\circ}$C) are required to produce increases in hardness. Thin foil electron microscopy has been used to check the structure of samples aged for times shorter than 10 minutes. It has been found that samples aged for 5 minutes at 900°F ($\sim 480^{\circ}$C) contain a low volume fraction of coarse ω-phase as shown in Figure 5. Apparently a low volume fraction, such as that shown in Figure 5, is insufficient to cause measurable hardening. This points out an obvious limitation of hardness data.

Oxygen also affects the kinetics of α-phase formation by increasing the rate at which it forms. This is in agreement with earlier work on the Ti-Mo binary system[17] and other binary and ternary systems.[4] These studies showed that increased oxygen promotes α-phase formation with the result that ω-phase is suppressed. Oxygen is generally agreed to be an α-phase stabilizer so this result is not surprising, although the details of how oxygen promotes α-phase formation are not clear. The variations in transformation kinetics of the low and high oxygen materials are summarized in the T-T-T curves of Figure 6.

Aging Temperature Effects

The aging temperature regime can be divided into those temperatures where the ω-phase forms and persists for extended period of time and those temperatures where α-phase forms as the predominant precipitate. Our results show that the ω-phase regime extends to $\sim$ 800°F ($\sim$ 425°C). Above this temperature α-phase predominates even though we have observed ω-phase in samples aged for short times at temperatures up to 900°F ($\sim$ 480°C).

Increasing the aging temperature within the temperature regime corresponding to ω-phase formation affects the incubation period which precedes any measurable increase in hardness, as can be seen in Figure 4. Two distinct factors may be important here. First, increasing the aging temperature between 400°F ($\sim$ 205°C) and 700°F ($\sim$ 370°C) reduces the time required to produce measurable hardening whereas further temperature increases above 700°F ($\sim$ 370°C) again increase the time to the onset of isothermal ω-phase formation. This is consistent with the normal C-curve behavior exhibited by nucleation and growth reactions, examples of these are shown in Figure 6. Second, from lever rule considerations, the metastable equilibrium volume fraction of ω-phase is reduced at temperatures >700°C ($\sim$ 370°C); · thus, the time required to form a sufficiently large ω-phase volume fraction to produce the observed hardening corresponds to a time for a larger percentage completion of the β→ω reaction.

There is also another aging temperature effect which is illustrated in Figure 4. This is the hardness plateau observed during the early stages of aging at 600°F ($\sim$ 315°C) and 800°F ($\sim$ 425°C) aging. Comparable effects are seen in the low oxygen material aged at 500°F ($\sim$ 260°C) and 600°F ($\sim$ 315°C).

It is curious that the 700°F ($\sim 370^{\circ}$C) aging curves for both oxygen levels do not exhibit any suggestion of the plateau.

Aging at temperatures above 800°F ($\sim 425^{\circ}$C) results in α-phase formation as mentioned earlier. The "nose" of the T-T-T curve for α-phase formation occurs at $\sim 1000^{\circ}$F ($\sim 535^{\circ}$C) as shown in Figure 6. Aging at various temperatures between 900°F ($\sim 480^{\circ}$C) and 1300°F ($\sim 705^{\circ}$C) results in α-phase precipitates ranging from very fine to coarse as shown in the series of replica electron micrographs in Figure 7. The size and spacing of the α-phase precipitates appears to qualitatively account for the variations in hardness shown earlier in Figure 4. The very coarse α-phase which forms at 1200°F ($\sim 650^{\circ}$C) and 1300°F ($\sim 705^{\circ}$C) does not cause any measurable hardness increase.[18]

Solution-Treatment Temperature Effects

The aging response has also been observed to depend on whether the solution-treatment temperature is above or below the $\beta/\alpha+\beta$ transformation temperature (commonly called the β-transus). The kinetics of β-phase decomposition during aging of the high oxygen material solution-treated above and below the β-transus and aged are summarized in the T-T-T curves, Figures 8(a) and (b). From these figures it can be seen that the α-phase precipitation occurs much more slowly in the material which was solution-treated above the beta-transus compared to the sub-transus solution-treated material. This solution temperature effect appears to be related to the occurrence of recovery and recrystallization with an attendant reduction in α-phase nucleation sites when the material is solution-treated above the β-transus. Dislocations and sub-boundaries act as strong nucleation sites as shown in Figure 9. This point is further demonstrated by the α-phase distribution in the partially recrystallized specimen shown in Figure 10.

The effect of solution-treatment temperature on ω-phase formation is also shown in Figures 8(a) and (b). From these figures, it can be seen that increasing the solution-treatment temperature to above the β-transus shifts the nose of the $\beta \rightarrow \omega + \beta$ C-curve to a higher temperature for the high oxygen material, but leaves it essentially unchanged in the low oxygen material. In both cases, the nose time is left virtually unaltered. The expected effect which accompanies a reduction in β-stabilizer content due to the increased solution-treatment temperature or a decrease in oxygen content is a broader temperature range for ω-phase formation. This is reflected in the upward shift of the $\beta \rightarrow \omega + \beta$ nose with increasing solution temperature in the high oxygen material. An even further shift is observed in the low oxygen material. The constancy of nose time is consistent with a transformation like the $\beta \overset{\rightarrow}{\leftarrow} \omega$ transformation for which there is a minimal barrier to nucleation so that heterogeneous nucleation does not significantly influence the transformation kinetics. This is in sharp contrast to the $\beta \overset{\rightarrow}{\leftarrow} \alpha$ transformation where the presence of heterogeneous nucleation sites in the sub-transus solution treated material was seen to markedly accelerate the reaction kinetics.

Direct Aging Studies

We have conducted a series of experiments in which the decomposition products and kinetics were examined as a function of thermal history. In these, samples quenched to room temperature from the solution-treatment temperature and then isothermally aged have been compared with samples taken directly from the solution-treatment temperature to the isothermal reaction temperature and held for a comparable length of time. We found that solution-treated and quenched samples aged for two hours at $800^{\circ}F$ ($\sim 425^{\circ}C$) exhibit extensive ω-phase formation whereas the samples directly aged at $800^{\circ}F$ ($\sim 425^{\circ}C$) for two hours ex-

hibited no ω-phase. This is illustrated in Figure 11. Comparison of additional samples held for 25 hours at 800°F ($\sim$ 425°C) showed that both the quenched and aged and the direct-aged samples contained ω-phase as shown in Figure 12. This increased incubation time in the direct aged material is consistent with the observed hardening response shown in Figure 13. Further, our observations of variation in incubation time with thermal history is somewhat analogous to observations in Al alloys[19] and some stainless steels.[20] In these latter systems it has been suggested that solute-vacancy complexes play a role in the nucleation process. Such complexes have never been suggested in connection with the $\beta \rightleftarrows \omega$ transformation but such a suggestion is one way to account for our observations.

Duplex Aging

We have also investigated several means of refining the α-phase precipitate size in an attempt to produce increased strengths for applications such as fasteners where the material is loaded in shear. One potential means of producing small, closely-spaced α-precipitates is to convert the ω-phase to α-phase by inducing an in-situ transformation. Other workers have shown that a coherent solvus exists for the ω-phase[21] and that temperature excursions above this solvus cause reversion of the ω-phase to solute-lean bcc zones not unlike β' mentioned earlier in this paper and described elsewhere.[2,4] Aging samples containing a $\beta+\omega$ mixture at temperatures at or just below the solvus temperature, results in the formation of fine α-phase, the scale of which distinctly resembles that of the ω-phase which concurrently disappears. Since both the ω and α-phases are solute-lean, it is reasonable to expect that the $\omega \rightleftarrows \alpha$ transformation is favorable since it has minimal diffusion requirements. There is still considerable question regarding the mechanism of transformation. Blackburn

and Williams[14] suggested that nucleation of α at $\beta:\omega$ interfaces occurs followed by growth of the α into the ω precipitate. There are several potential difficulties attendant with this interpretation, the most important of which is that only four α-phase variants are predicted but more are observed. Moreover, the predicted orientation relation is wrong. Nevertheless, we have observed anomalous fringe contrast at ω-phase particles in duplex aged (low + high) specimens as seen in Figure 14. These fringes are not observed in samples containing $\beta+\omega$ thus the appearance of these fringes may be related to the presence of a thin α-phase platelet but this point has not been proved conclusively. Irrespective of this, duplex (low + high) aging treatments result in high strengths and limited ductility as shown in Table II.

Cold Work + Aging Treatments

Several specimen of high oxygen material were solution treated above the β-transus, quenched, cold worked 10% and aged at 700°F ($\sim 370^{\circ}$C) for various times. The hardness-time curves obtained from these samples are shown in Figure 15. From these curves it can be seen that cold work prior to aging accelerates the aging response. Thin foil electron microscopy examination of these specimens showed that the cold worked and aged samples contain a mugh higher volume fraction of ω-phase when compared to samples which were quenched and aged. This is illustrated in Figure 16(a) and (b) and in Figure 17(a) and (b). The reasons for the acceleration of ω-phase formation are not completely understood, however, we point out that this observation is also consistent with vacancy aided nucleation suggested earlier. If room temperature cold work creates vacancies, then the vacancy concentration of the cold worked samples would be greater than the quenched and aged samples leading to higher nucleation rates. Again, it should be recognized that the evidence we present for the role of vacancies, in ω-phase nucleation is not conclusive but does form a self-consistent pattern.

The foregoing results illustrate the importance of selecting proper combinations of solution treatment and aging temperatures if the ω-phase is to be avoided. Super-transus solution treatment should be avoided because it removes the heterogeneous nucleation sites which accelerate the rate of formation of α-phase relative to that of ω-phase. Duplex (low-high) aging has no advantage with regard to strengthening potential in sub-transus solution treated material; in super-transus solution treated material, the potential advantage of duplex aging is much greater. Finally the effect of quench history and varying amounts of cold work on the kinetic balance between ω-phase and α-phase formation are interesting because they suggest additional ways of controlling ω-phase formation. Further studies in this area appear to be warranted.

SUMMARY AND CONCLUSIONS

In summary, we have found that the microstructure and hardening response of Ti-11.5Mo-6Zr-4.5Sn (β-III) depends on quenching history on solution treatment temperature, on aging time and temperature and on oxygen content of the alloy. Specifically, we have observed the following.

1. The ω-phase forms on aging at temperatures up to 900°F
   ($\sim 480^{\circ}$C) although at 900°F it has a limited time of
   stability.

2. In recovered and incompletely recrystallized material
   heterogeneous nucleation of α-phase occurs at dislocations
   and sub-boundaries whereas ω-phase is uniformly nucleated
   in the matrix.

3. The hardening due to ω-phase formation exhibits very little
   overaging response as long as ω-phase is present.

4. The incubation time for ω-phase formation is substantially
   lengthened in directly aged samples compared to quenched and
   aged samples.

5. There is a critical α-phase particle size and spacing above which only very limited hardening is observed.

6. Increasing oxygen content accelerates the kinetics of α-phase formation and retards those of ω-phase formation.

7. Cold working prior to aging in the ω-phase range accelerates formation of ω-phase.

8. Duplex aging at low temperatures and then at high temperatures results in very fine α-phase particles, possibly due to an in-situ $\omega \rightarrow \alpha$ transformation.

9. A hardening plateau was observed during the early stages of aging at lower temperatures. The reason for this plateau was not determined.

ACKNOWLEDGEMENTS

REFERENCES

1. J. B. Guernsey, SAE Transactions, 29, 2540 (1970).

2. J. C. Williams, "Titanium Science and Technology," Jaffee and Burte, Eds. Vol 3, p 1433, Plenum Press, N.Y., 1973.

3. C. G. Rhodes and J. C. Williams, Met. Trans., 6A, 2103 (1975).

4. J. C. Williams, B. S. Hickman and D. H. Leslie, Met. Trans., 2, 1913 (1971).

5. J. M. Silcock, Acta Met., 6, 481 (1958).

6. B. S. Hickman, Jnl. Mat'ls. Science, 4, 554 (1969).

7. M. J. Blackburn and J. C. Williams, Trans (Met. Soc.) AIME, 242, 2461 (1968).

8. E. L. Harmon and A. R. Troiano, Trans ASM, 53, 43 (1961).

9. J. C. Williams, B. S. Hickman and H. L. Marcus, Met. Trans., 2, 1913 (1971).

10. P. Ganesau, R. J. De Angelis and Gordon A. Sargent, Jl. Less Comm. Metals, 34, 209 (1974).

11. V. C. Petersen, F. H. Froes and R. F. Malone, same as reference 2, Vol 3, p 1969.

12. F. H. Froes, J. M. Capenos and M.G.H. Wells, ibid, Vol 3, p 1622.

13. L. A. Rosales, Ph.D. Thesis, U.C.L.A., 1970.

14. M. J. Blackburn and J. C. Williams, Trans. (Met Soc.) AIME, 239, 287 (1967).

15. R. A. Spurling, C. G. Rhodes and J. C. Williams, Met. Trans., 5, 2597 (1974).

16. N. E. Paton and J. C. Williams, Scripta Met., 7, 647 (1973).

17. D. J. Delazaro and W. Rostoker, Acta Met., 1, 674 (1953).

18. F. H. Froes, R. F. Malone, V. C. Petersen, C. G. Rhodes, J. C. Chesnutt and J. C. Williams, AFML-TR-75-41, September 1975.

19. A. Kelly and R. B. Nicholson, Prog.Mat.Sci., 10, 151 (1963).

20. F. H. Froes, B. R. Banerjee and M.G.H. Wells, Met. Sci. Jnl., 2, 232 (1968).

21. See for example, R. R. Boyer, M.S. Thesis, University of Washington, 1972.

TABLE I

CHEMICAL ANALYSIS OF BETA III HEATS

	Mo wt pct	Zr wt pct	Sn wt pct	Fe wt pct	H wt pct	O wt pct	N wt pct	C wt pct
Low Oxygen	11.30	6.17	4.38	0.02	0.0034	<u>0.17</u>	0.013	0.02
High Oxygen	11.52	5.22	4.27	0.03	0.0087	<u>0.28</u>	0.017	0.03

TABLE II

MECHANICAL PROPERTIES OF 0.060 inch BETA III SHEET

Heat Treatment Type	Aging Treatments[a] I Temp. °F(°C)	I Time (hr)	II Temp. °F(°C)	II Time (hr)	Dirn.[b]	Tensile Properties UTS (ksi)	YS (ksi)	El (%)	RA (%)	E (x10^6 psi)
α	-	-	950 (510)	8	L	192.2	179.2	6.5	19.9	14.7
			950 (510)	8	T	195.7	184.4	5.0	18.5	15.3
ω + α	700 (370)	0.33	950 (510)	8	L	200.7	193.4	5.0	21.8	14.4
					T	179.7	170.1	4.0	18.0	14.0
ω + α	700 (370)	50	950 (510)	8	L	202.4	194.6	5.5	25.7	16.7
					T	191.4	177.7	4.5	18.0	16.3

1 ksi = 6.89 MPa

[a] After a 1325F (720C) - 5 min. solution treatment and water quench.

[b] L: longitudinal; T: transverse.

FIGURE CAPTIONS

Figure 1:   Variation of hardness with aging time at 700°F (370°C) for
             Beta III containing two oxygen levels and solution treated
             above the beta transus.

Figure 2:   Thin foil electron micrograph and selected area diffraction
             pattern illustrating the presence and distribution of athermal
             omega phase in Beta III (0.28% O_2) quenched from 1650°F (900°C).

   (a) Dark field micrograph taken using a $(10\bar{1}1)_\omega$ reflection.

   (b) Selected area electron diffraction pattern showing diffuse
        omega reflection and streaking. $<110>_\beta$ zone normal.

Figure 3:   Dark field electron micrographs showing coarsening of omega phase
             during aging of 0.28% oxygen material quenched from 1650°F (900°C)
             and aged at 700°F (370°C).

   (a) 8 h age.   (b) 500 h age.

Figure 4:   Variation of hardness with aging time for Beta III (0.28% O_2)
             solution treated at 1650°F (900°C), water quenched and aged at
             the indicated temperature.

Figure 5:   Dark field electron micrograph showing a low volume fraction of
             coarse ellipsoidal omega phase and a high volume fraction of
             fine omega phase in Beta III (0.28% O_2) quenched from 1650°F (900°C)
             and aged 5 min. at 900°F (~480°C).

Figure 6:   Isothermal transformation diagrams for 0.28% O_2 and 0.17% O_2
             Beta III, showing effect of oxygen on the beta $\rightarrow$ omega and
             beta $\rightarrow$ alpha reactions in material quenched from 1650°F (900°C).

Figure 7: Replica electron micrographs showing the distribution of alpha phase precipitates in 0.28% O_2 Beta III aged 8 hours at the following temperatures.

(a) 900^oF ($\sim 480^o$C) (b) 1000^oF ($\sim 535^o$C)

(c) 1100^oF ($\sim 595^o$C) (d) 1300^oF ($\sim 705^o$C)

Figure 8: Isothermal transformation diagrams for 0.17% O_2 and 0.28% O_2 Beta III solution annealed above and below the beta transus, the actual temperatures are indicated on diagrams.

(a) 0.28% O_2 material (b) 0.17% O_2 material

Figure 9: Bright field and dark field electron micrographs showing preferential nucleation of alpha phase at dislocations in Beta III quenched from 1650^oF (900^oC) and aged 5 min. at 900^oF ($\sim 480^o$C).

(a) Bright field. (b) Dark field, $(10\bar{1}1)$ reflection.

Figure 10: Replica electron micrograph showing variation in alpha phase precipitate size and distribution in recrystallized and unrecrystallized regions of Beta III (0.28% O_2). Material was solution treated for 5 min. at 1500^oF (815^oC), quenched and aged 30 min. at 1100^oF ($\sim 595^o$C).

Figure 11: Bright field electron micrograph and selected area electron diffraction pattern showing the effect of direct aging on decomposition kinetics of Beta III (0.28% O_2). Sample was solution treated at 1650^oF (900^oC) and directly aged at 800^oF ($\sim 425^o$C) for 2 h.

(a) Micrograph showing grain boundary nucleated alpha phase.

(b) Diffraction pattern showing absence of sharp omega phase reflections of the type associated with isothermally formed omega phase.

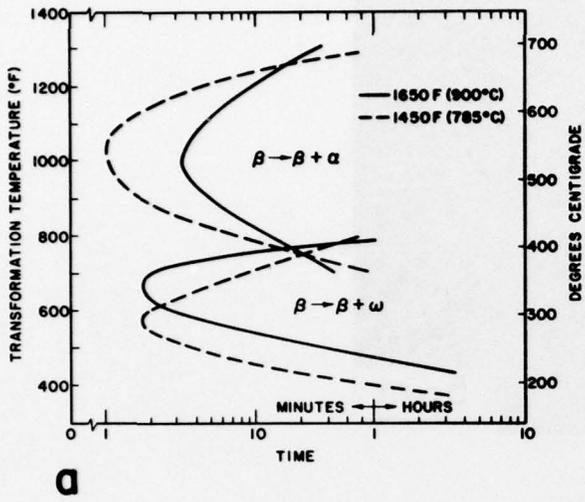Figure 3

Figure 4

Figure 5

Figure 6

a 5μm

b 5μm

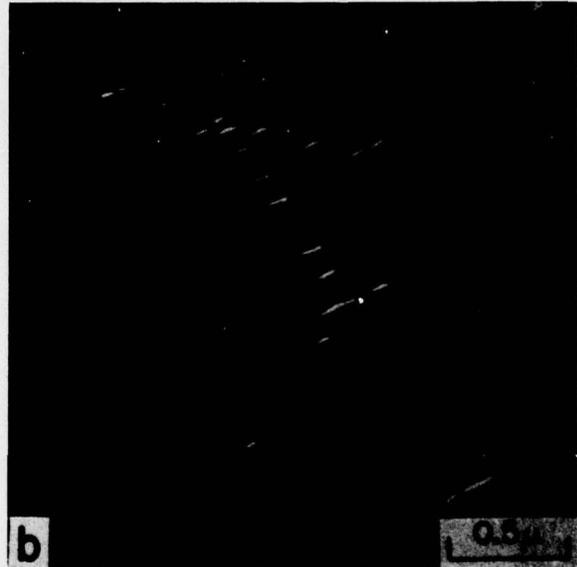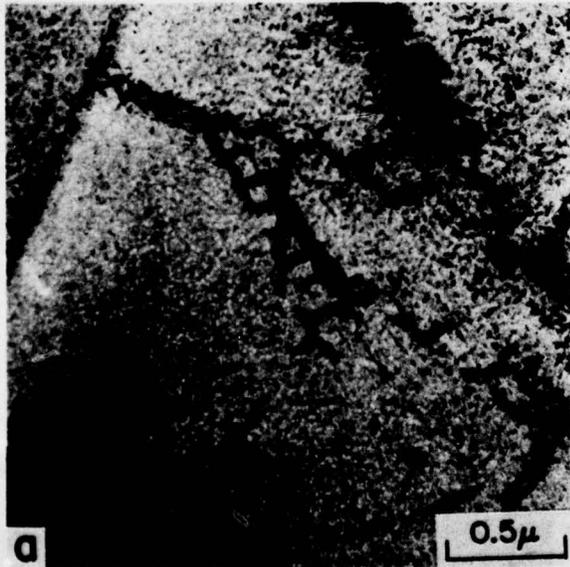c 5μm

d 5μm

Figure 7

Figure 8

Figure 9

5μm

Figure 10

0.5μ

a   b

Figure 11
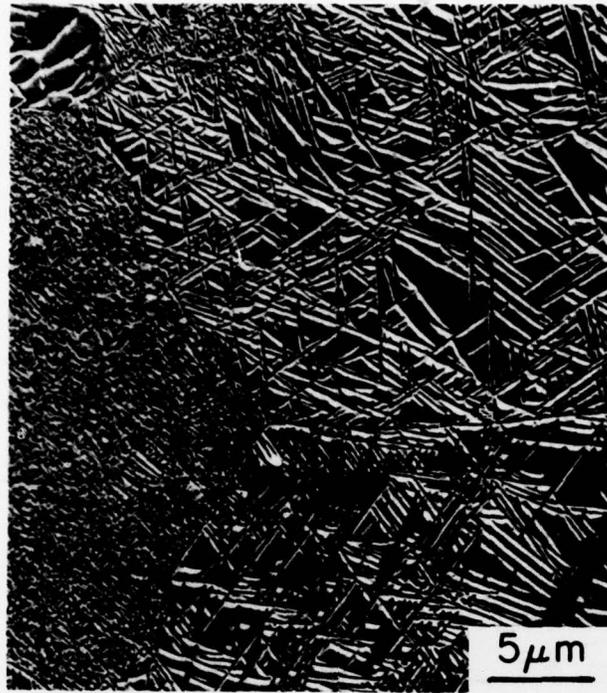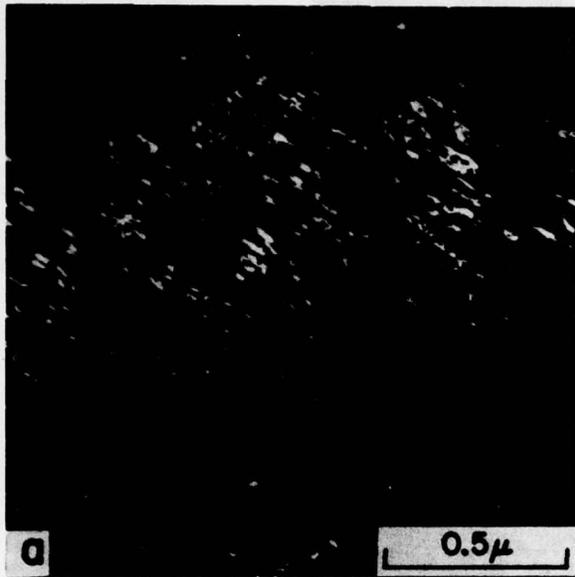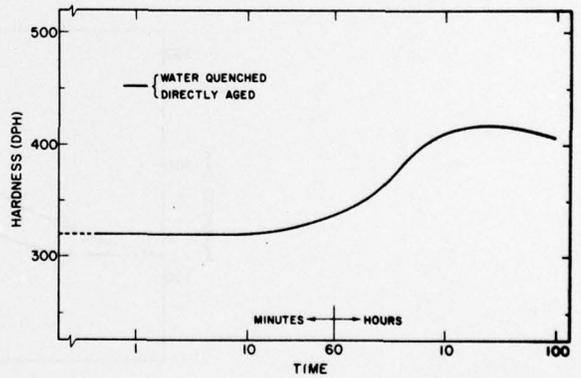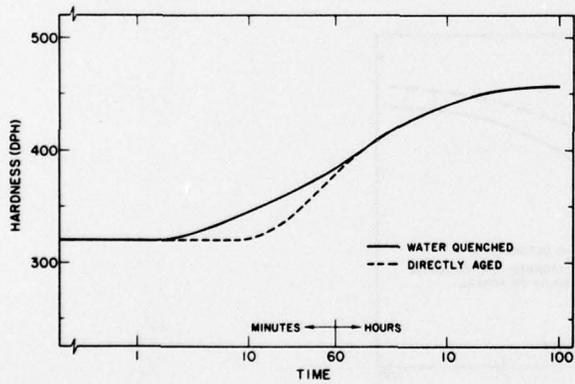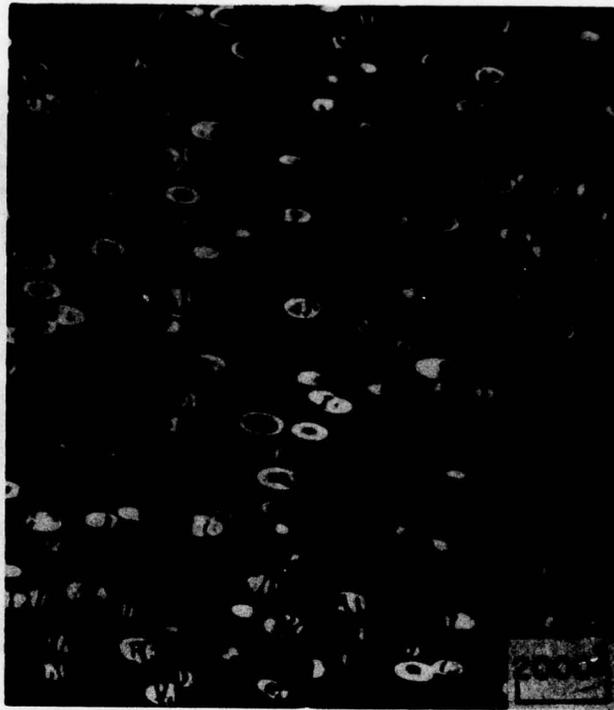
Figure 12

Figure 13

Figure 14
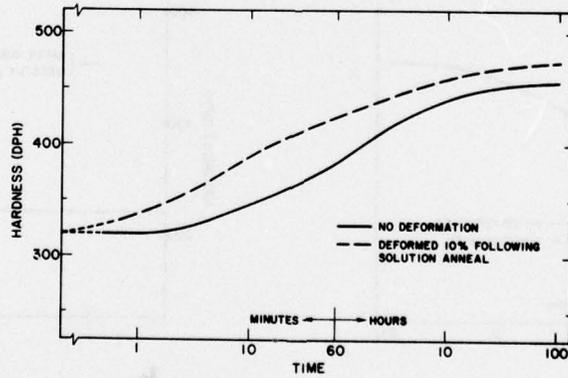
Figure 15
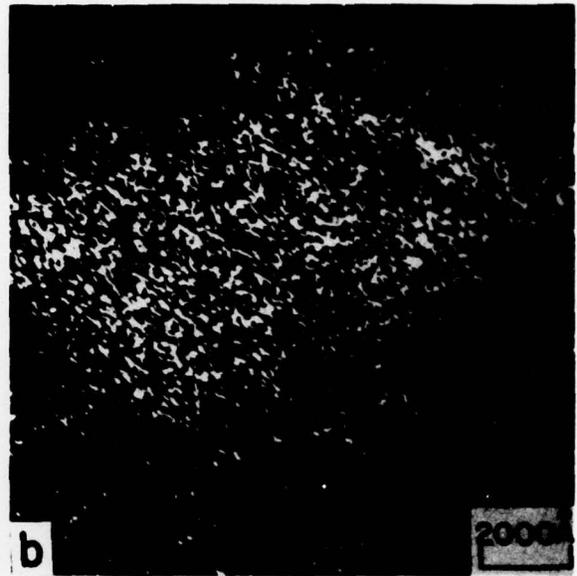
Figure 16

Figure 17

DOCUMENT CONTROL DATA - R&D

(Security classification of title, body of abstract and indexing annotation must be entered when the overall report is classified)

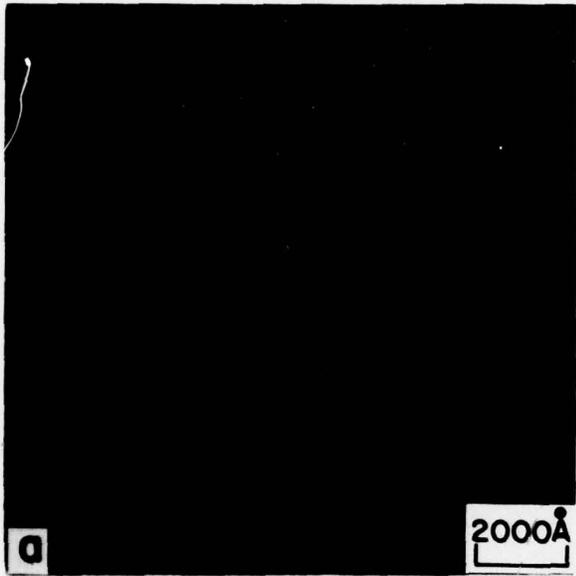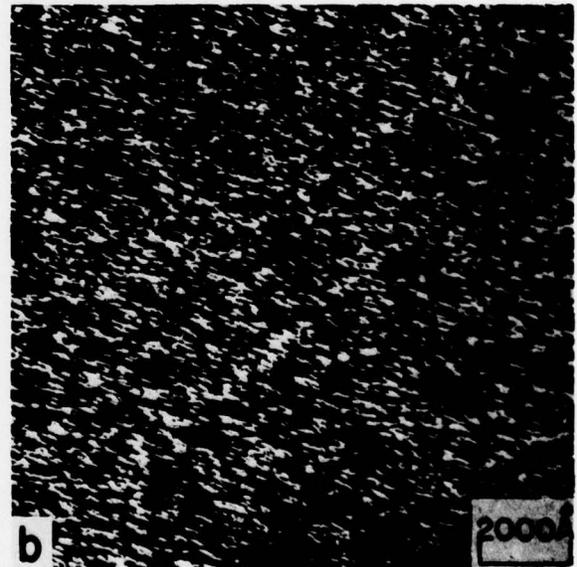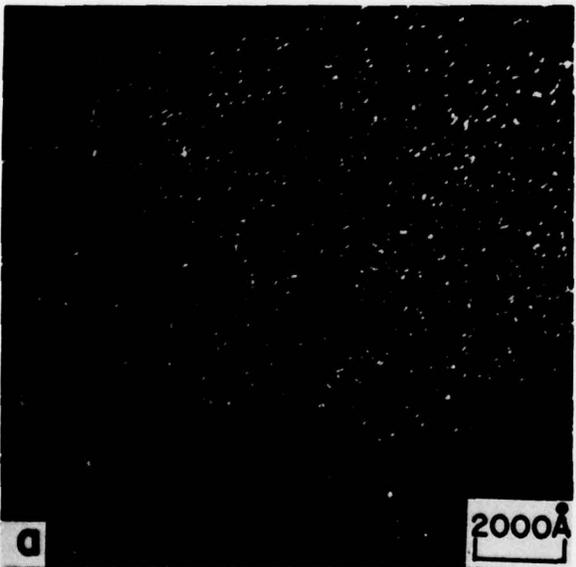| 1. ORIGINATING ACTIVITY (Corporate author)	2a. REPORT SECURITY CLASSIFICATION
Carnegie-Mellon University	Unclassified
	2b. GROUP ----

3. REPORT TITLE

The Relationship Between the Microstructure and Age Hardening Response in the Metastable β Titanium Alloy Ti-11.5Mo-6Zr-4.5Sn (Beta III).

4. DESCRIPTIVE NOTES (Type of report and inclusive dates)

Technical Report.

5. AUTHOR(S) (Last name, first name, initial)

Froes, F. H.; Yolton, J. M.; Wells, M. G. H.; Williams, J. C.

6. REPORT DATE	7a. TOTAL NO. OF PAGES	7b. NO. OF REFS
Aug. 1977	26	21

8a. CONTRACT OR GRANT NO.	9a. ORIGINATOR'S REPORT NUMBER(S)
N00014-76-C-0409	JWTR-3
b. PROJECT NO.	
c.	9b. OTHER REPORT NO(S) (Any other numbers that may be assigned this report)
d.	-----

10. AVAILABILITY/LIMITATION NOTICES

Unlimited

11. SUPPLEMENTARY NOTES	12. SPONSORING MILITARY ACTIVITY
To be published in Met Trans	Office of Naval Research

13. ABSTRACT

The effect of solution treatment temperature and oxygen content on the microstructure and age hardening response of the metastable β alloy Ti-11.5Mo-6Zr-4.5Sn have been studied. Kinetics of formation of the equilibrium α-phase and the metastable ω-phase have been followed using Vicker's hardness measurements. These kinetics have been examined as a function of solution treatment temperature (above or below the β-transus) and initial oxygen of the material. It has been found that the kinetics of formation of ω-phase are relatively insensitive to these variables whereas α-phase is quite sensitive. The effect of these variables on microstructure has been evaluated using light microscopy, replica electron microscopy and thin foil transmission electron microscopy. Several duplex aging treatments starting in the ω-phase temperature range and finishing in the α-phase temperature range were also examined. TEM of these samples has provided some inside into the mechanism of the ω→α in-situ transformation.

404459

14. KEY WORDS	LINK A		LINK B		LINK C	
	ROLE	WT	ROLE	WT	ROLE	WT
Electron microscopy, Titanium alloys, Age Hardening						

INSTRUCTIONS

1. **ORIGINATING ACTIVITY:** Enter the name and address of the contractor, subcontractor, grantee, Department of Defense activity or other organization (*corporate author*) issuing the report.

2a. **REPORT SECURITY CLASSIFICATION:** Enter the overall security classification of the report. Indicate whether "Restricted Data" is included. Marking is to be in accordance with appropriate security regulations.

2b. **GROUP:** Automatic downgrading is specified in DoD Directive 5200.10 and Armed Forces Industrial Manual. Enter the group number. Also, when applicable, show that optional markings have been used for Group 3 and Group 4 as authorized.

3. **REPORT TITLE:** Enter the complete report title in all capital letters. Titles in all cases should be unclassified. If a meaningful title cannot be selected without classification, show title classification in all capitals in parenthesis immediately following the title.

4. **DESCRIPTIVE NOTES:** If appropriate, enter the type of report, e.g., interim, progress, summary, annual, or final. Give the inclusive dates when a specific reporting period is covered.

5. **AUTHOR(S):** Enter the name(s) of author(s) as shown on or in the report. Enter last name, first name, middle initial. If military, show rank and branch of service. The name of the principal author is an absolute minimum requirement.

6. **REPORT DATE:** Enter the date of the report as day, month, year; or month, year. If more than one date appears on the report, use date of publication.

7a. **TOTAL NUMBER OF PAGES:** The total page count should follow normal pagination procedures, i.e., enter the number of pages containing information.

7b. **NUMBER OF REFERENCES:** Enter the total number of references cited in the report.

8a. **CONTRACT OR GRANT NUMBER:** If appropriate, enter the applicable number of the contract or grant under which the report was written.

8b, 8c, & 8d. **PROJECT NUMBER:** Enter the appropriate military department identification, such as project number, subproject number, system numbers, task number, etc.

9a. **ORIGINATOR'S REPORT NUMBER(S):** Enter the official report number by which the document will be identified and controlled by the originating activity. This number must be unique to this report.

9b. **OTHER REPORT NUMBER(S):** If the report has been assigned any other report numbers (*either by the originator or by the sponsor*), also enter this number(s).

10. **AVAILABILITY/LIMITATION NOTICES:** Enter any limitations on further dissemination of the report, other than those imposed by security classification, using standard statements such as:

(1) "Qualified requesters may obtain copies of this report from DDC."

(2) "Foreign announcement and dissemination of this report by DDC is not authorized."

(3) "U. S. Government agencies may obtain copies of this report directly from DDC. Other qualified DDC users shall request through

_____."

(4) "U. S. military agencies may obtain copies of this report directly from DDC. Other qualified users shall request through

_____."

(5) "All distribution of this report is controlled. Qualified DDC users shall request through

_____."

If the report has been furnished to the Office of Technical Services, Department of Commerce, for sale to the public, indicate this fact and enter the price, if known.

11. **SUPPLEMENTARY NOTES:** Use for additional explanatory notes.

12. **SPONSORING MILITARY ACTIVITY:** Enter the name of the departmental project office or laboratory sponsoring (*paying for*) the research and development. Include address.

13. **ABSTRACT:** Enter an abstract giving a brief and factual summary of the document indicative of the report, even though it may also appear elsewhere in the body of the technical report. If additional space is required, a continuation sheet shall be attached.

It is highly desirable that the abstract of classified reports be unclassified. Each paragraph of the abstract shall end with an indication of the military security classification of the information in the paragraph, represented as *(TS)*, *(S)*, *(C)*, or *(U)*.

There is no limitation on the length of the abstract. However, the suggested length is from 150 to 225 words.

14. **KEY WORDS:** Key words are technically meaningful terms or short phrases that characterize a report and may be used as index entries for cataloging the report. Key words must be selected so that no security classification is required. Identifiers, such as equipment model designation, trade name, military project code name, geographic location, may be used as key words but will be followed by an indication of technical context. The assignment of links, roles, and weights is optional.